Highly Dispersed Networks Generated by Enhanced Redirection

Alan Gabel[1], **P L Krapivsky**[1], **and S Redner**[1,2]

[1]Department of Physics, Boston University, Boston, Massachusetts 02215, USA

[2]Santa Fe Institute, 1399 Hyde Park Road, Santa Fe, New Mexico 87501, USA

Abstract. We analyze growing networks that are built by enhanced redirection. Nodes are sequentially added and each incoming node attaches to a randomly chosen 'target' node with probability $1-r$, or to the parent of the target node with probability r. When the redirection probability r is an increasing function of the degree of the parent node, with $r \to 1$ as the parent degree diverges, networks grown via this *enhanced* redirection mechanism exhibit unusual properties, including: (i) multiple macrohubs, i.e., nodes with degrees proportional to the number of network nodes N; (ii) non-extensivity of the degree distribution in which the number of nodes of degree k, N_k, scales as $N^{\nu-1}/k^{\nu}$, with $1 < \nu < 2$; (iii) lack of self-averaging, with large fluctuations between individual network realizations. These features are robust and continue to hold when the incoming node has out-degree greater than 1 so that networks contain closed loops. The latter networks are strongly clustered; for the specific case of double attachment, the average local clustering coefficient is $\langle C_i \rangle = 4 \ln 2 - 2 = 0.77258\ldots$.

PACS numbers: 02.50.Cw, 05.40.-a, 05.50.+q, 87.18.Sn

1. Introduction

Models for the growth of complex networks often involve mechanisms that are based on *global* knowledge of the network. For example, in preferential attachment [1–7], nodes are added sequentially and each links to existing target nodes in the network according to an attachment rate A_k that is an increasing function of the degree k of the target node. According to this rule, incoming nodes must 'know' the degree distribution of the entire network to correctly choose a target node. In real networks, however, it is not feasible that any new node has such detailed global knowledge.

The impracticality of implementing a growth rule based on global knowledge has motivated alternatives to preferential attachment that rely on the incoming nodes exploiting only *local* knowledge of a small portion of the network. Examples include attachment via spatial locality [8–10] and node similarity [11]. In this work, we focus on the local growth rule that exploits *redirection* [12–18]. Here, each incoming node selects a target node at random and links either to this target node (probability $1-r$), or to parent of the target node (probability r). This redirection rule is based on the network being directed so that the parent(s) of any node is well defined. If each new node has only one outgoing link, redirection produces networks with a tree topology; it is straightforward to extend redirection to allow each incoming node to attach to more than one node in the network [15].

The surprising feature of redirection with a fixed redirection probability r is that it is mathematically equivalent to the global growth rule of shifted linear preferential attachment, where the rate of attaching a new node to a pre-existing node of degree k is $A_k = k+\lambda$ with $\lambda = r^{-1}-2$, see [13]. Redirection is also highly efficient because one only needs to select a random node and identify its parent to add a node to the network. The time to create a network of N nodes via redirection therefore scales linearly with N.

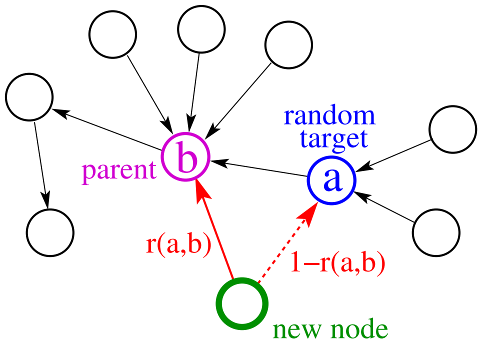

Figure 1. Illustration of enhanced redirection. The redirection probability $r(a,b)$ depends on the degree a of a randomly chosen target node and the degree b of its parent, with $r(a,b)$ an increasing function of b and $r\to 1$ as $b\to\infty$. In this example, the degree of the parent node is large, so the new node is likely to attach to the parent.

The utility of redirection as a simple and efficient procedure that is equivalent to linear preferential attachment motivates us to exploit models that use slightly more comprehensive (but still local) degree information around the target node. Specifically we allow the redirection probability $r(a, b)$ to depend on the degrees of the target and parent nodes, a and b respectively (Fig. 1). In *hindered redirection*, $r(a, b)$ is a decreasing function of the parent degree b, a rule that leads to sub-linear preferential attachment growth [19]. In this work, we investigate the complementary situation of *enhanced redirection*, for which the redirection probability r is an increasing function of the parent degree b, with $r \to 1$ as $b \to \infty$. This seemingly-innocuous redirection rule gives rise to networks with several intriguing and practically relevant properties:

(i) ***Appearance of multiple macrohubs*:** Macrohubs are nodes whose degrees are a finite fraction of N. While macrohubs arise in other models [4, 13, 20–22], the resulting networks are singular, with nearly all nodes attached to a single macrohub. In the cases of superlinear preferential attachment, where $A_k \sim k^\gamma$ with $\gamma > 1$ [4,13,20], and in the fitness model, where the attachment rate is proportional to both the degree k and fitness of the target [22, 23], a single macrohub arises that is connected to almost all other nodes of the network. In contrast, enhanced redirection networks are highly disperse (Fig. 2), with interconnected hub-and-spoke structures that are reminiscent of airline route networks [7, 21, 24–26].

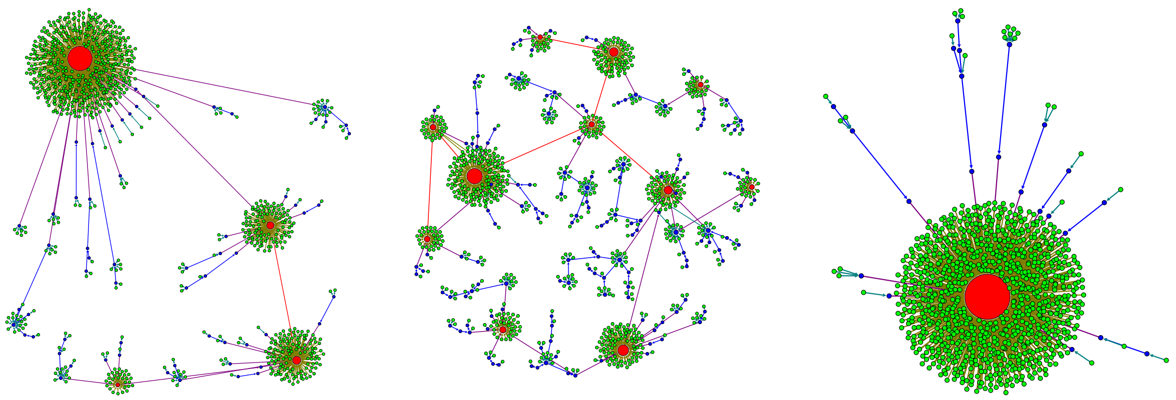

(a) (b) (c)

Figure 2. Enhanced redirection networks of $N = 10^3$ nodes for $\lambda = \frac{3}{4}$ (see Eq. (3)) starting from the same initial state. (a) Maximum degree $k_{\max} = 548$, $\mathcal{C} = 66$ core ($k \geq 2$) nodes, and maximum depth $D_{\max} = 10$. (b) $k_{\max} = \mathcal{C} = 154$, $D_{\max} = 12$ (smallest $k_{\max}$ out of 10^3 realizations). (c) $k_{\max} = 963$, with $\mathcal{C} = 23$ and $D_{\max} = 6$ (largest $k_{\max}$ out of 10^3 realizations). Green: nodes of degree 1, blue: degrees 2–20, red: degree > 20. The link color is the average of the endpoint node colors.

(ii) ***Non-extensivity*:** In many sparse networks, the degree distribution is extensive, with the number of nodes of degree k, N_k, proportional to N. This happens, for example, in linear preferential attachment where additionally the degree distribution has an algebraic tail, $N_k \sim N/k^\nu$ for $k \gg 1$, with $\nu > 2$. In contrast, enhanced redirection leads to the non-extensive scaling

$$N_k \sim \frac{N^{\nu-1}}{k^\nu} \qquad \text{with} \quad \nu < 2. \tag{1}$$

The allowed range of the exponent ν is key. While past empirical studies have observed networks with degree exponent in the range $1 < \nu < 2$ [27] (see Table 1 for some examples), the range $1 < \nu < 2$ is mathematically inconsistent for sparse networks because it leads to a divergent average degree as $N \to \infty$ whenever the degree distribution obeys the standard scaling $N_k \sim Nk^{-\nu}$. A simple resolution of this dilemma is to relax the hypothesis of extensivity. We shall see that in enhanced redirection almost all nodes have degree 1 (leaves). More precisely, the number $\mathcal{C} \equiv N - N_1$ of core nodes (nodes with degree > 1) grows *sub-linearly* with N, namely as $N^{\nu-1}$ with the exponent ν in the range $1 < \nu < 2$. All N_k with $k \geq 2$ also grow as $N^{\nu-1}$. This anomalous scaling can therefore be summarized as follows:

$$\mathcal{C} = N - N_1 \simeq c_1 N^{\nu-1}\,, \qquad N_k \simeq c_k N^{\nu-1} \quad \text{for} \quad k \geq 2 \tag{2}$$

where c_k are constants. This scaling satisfies the sum rule $\sum_{1\leq k\leq N} N_k = N$ and leads to a finite average degree $\langle k \rangle$ without imposing an artificial cutoff in the degree distribution.

Network	exponent ν	average degree	network size
Orkut	1.27	76.281	3,072,441
Catster Friendships	1.36	72.803	149,700
Dogster Friendships	1.40	40.048	426,820
arXiv hep-ph	1.47	224.14	28,093
arXiv hep-th	1.47	213.44	22,908
Wikipedia conflict	1.50	34.644	118,100
Hamsterster full	1.52	13.711	16,630
Hamsterster Friendships	1.54	13.491	1,858
Flickr	1.73	43.742	105,938
Internet topology	1.86	9.8618	34,761
Wikipedia, Italian	1.48	28.457	1,204,009
Wikipedia, German	1.50	28.811	2,166,669
LiveJournal	1.56	28.465	4,847,571
Wikipedia, French	1.62	22.165	2,212,682
OpenFlights	1.79	20.756	2,939

Table 1. Networks with degree exponent $\nu < 2$. All examples are simple graphs (at most one link between any node pair); the first 10 are undirected and the remainder are directed. Data at http://konect.uni-koblenz.de/networks.

(iii) ***Lack of self-averaging***: Different realizations of enhanced redirection are visually diverse when starting from the same initial condition (Fig. 2). Basic network measures, such as the number of nodes of fixed degree, N_k with any $k \geq 2$, or the number of core nodes $\mathcal{C}$, vary significantly between realizations and do not converge as $N \to \infty$. For instance, the ratio of the mean deviation to the average, $\sqrt{\langle \mathcal{C}^2 \rangle - \langle \mathcal{C} \rangle^2}/\langle \mathcal{C} \rangle$, converges to a positive constant when $N \to \infty$, thereby manifesting the lack of self-averaging. In contrast, preferential attachment networks do self-average, as the relative deviations in N_k or $\mathcal{C}$ systematically decrease as N increases [28].

In the next section we formally define our enhanced redirection models. In Sect. 3 we provide analytical and numerical arguments that justify the properties (i), (ii), (iii) given above. Some of these arguments substantially extend our findings that were reported in Ref. [29]. Most results in Sect. 4, and all results in Sect. 5 about enhanced redirection with multiple attachments, are new.

2. Enhanced Redirection Model

We define the initial network to be a single node that is linked to itself, so that the root node is its own parent and its own child. The initial conditions have a weak and mostly quantitative influence on asymptotic network properties. Thus we shall generally use the above simple initial condition; we will explicitly define other initial conditions in the few cases where such a modification is more amenable to analysis.

Links are directed so that the parent and children of any node are well defined. In Sects. 3–4 we investigate models in which each node has out-degree equal to 1, and thus a unique parent. This growth rule produces tree networks if the starting network is a tree. Our networks are trees with the exception of the initial self loop.

Nodes are introduced one by one. Each incoming node first picks a random target node. If the degrees of the target and parent nodes are a and b, respectively, then the new node (see Fig. 1)

(i) attaches to the target with probability $1 - r(a, b)$;
(ii) or attaches to the parent of the target with probability $r(a, b)$.

Two natural (but by no means unique) choices for the redirection probability are

$$r(a, b) = 1 - b^{-\lambda}, \qquad r(a, b) = \frac{a^\lambda}{a^\lambda + b^\lambda}, \qquad \lambda > 0 . \tag{3}$$

Our results are robust with respect to the form of the redirection probability, as long as $r(a, b) \to 1$ as $b \to \infty$. For concreteness, we focus on the redirection probability $r(a, b) = 1 - b^{-\lambda}$. In Appendix A we compare some results for this case with corresponding results for the redirection probability $r(a, b) = a^\lambda/(a^\lambda + b^\lambda)$. This comparison indicates that the two models are qualitatively the same.

3. Degree Distribution and Lack of Self-Averaging

We first study the degree distribution $\langle N_k \rangle$, the average number of nodes of degree k; to avoid notational clutter we drop the angle brackets henceforth. Simulation results clearly show that the degree distribution has the anomalous scaling behaviors given by Eq. (2) (Fig. 3). The exponent ν depends on the redirection parameter λ, but is always less than 2 (Fig. 4) so that the degree distribution decays very slowly in k. Because $\nu < 2$, Eq. (2) implies that the number of nodes of degree 1 grow more rapidly with N than the number of core nodes. Thus, visually, a typical network is dominated by its leaves.

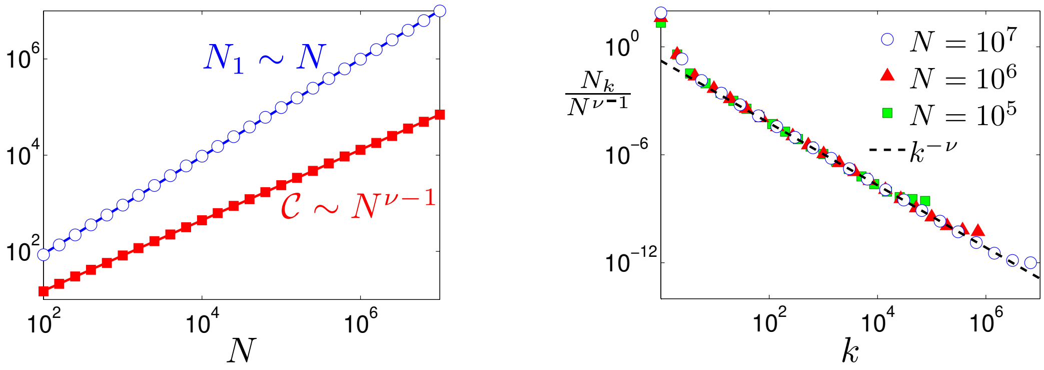

(a) (b)

Figure 3. (a) N_k versus N and (b) $N_k/N^{\nu-1}$ versus k for enhanced redirection with $\lambda = \frac{3}{4}$ and $\nu = 1.73$ (determined numerically; see Fig. 4). Data are based on 10^4 realizations, with equally-spaced bins on a logarithmic scale in (b). The lines in (a) show the prediction of Eq. (2), while the line in (b) shows the k dependence from the numerical solution of (8).

We employ the master equation approach to understand the anomalous scaling in Eq. (2). The degree distribution evolves according to

$$\frac{dN_k}{dN} = \frac{(1-f_{k-1})N_{k-1} - (1-f_k)N_k}{N} + \frac{(k-2)t_{k-1}N_{k-1} - (k-1)t_k N_k}{N} + \delta_{k,1}\,. \qquad (4)$$

Here f_k and t_k are defined as the respective probabilities that an incoming link is redirected *from* a node of degree k, and redirected *to* a node of degree k. The first ratio in Eq. (4) accounts for instances in which the incoming node attaches directly to the target node. Thus the term $(1 - f_k)N_k/N$ gives the probability that the randomly selected target node has degree k and the incoming node is *not* redirected. The term is negative because the target node degree increases from k to $k + 1$ which causes N_k to decrease. Similarly, the second ratio corresponds to instances in which the incoming node is redirected to the parent. Thus the term $(k - 1)t_k N_k/N$ gives the probability that one of the $(k-1)N_k$ children of a degree k node is targeted and that the incoming node is redirected to the parent. The term $\delta_{k,1}$ arises because each newly added node has degree 1.

The probabilities f_k and t_k are defined by

$$f_k = \sum_{b\geq 1} \frac{r(k,b)N(k,b)}{N_k}\,, \qquad\qquad t_k = \sum_{a\geq 1} \frac{r(a,k)N(a,k)}{(k-1)N_k}\,. \tag{5}$$

Here the correlation function $N(a,b)$ is defined as the number of nodes of degree a that have a parent of degree b. Thus f_k is the probability of redirecting *from* a node of degree k, averaged over all such target nodes, and t_k is the probability of redirecting *to* a node of degree k, averaged over all the $(k-1)N_k$ children of nodes of degree k. Defining $\alpha_k = (k-1)t_k + 1 - f_k$, Eq. (4) can be written in the canonical form

$$\frac{dN_k}{dN} = \frac{\alpha_{k-1}N_{k-1} - \alpha_k N_k}{N} + \delta_{k,1}\,. \tag{6}$$

Substituting Eq. (2) into the master equations (4) gives the recursions:

$$\begin{aligned}
(\nu-1)c_1 N^{\nu-2} &= \alpha_1\big(1 - c_1 N^{\nu-2}\big) && k=1\\
(\nu-1)c_2 N^{\nu-2} &= \alpha_1\big(1 - c_1 N^{\nu-2}\big) - \alpha_2 c_2 N^{\nu-2} && k=2\\
c_k &= \frac{\alpha_{k-1}}{\alpha_k + \nu - 1}\, c_{k-1} && k\geq 3\,.
\end{aligned} \tag{7}$$

We eliminate the common factor in the first two lines to obtain $c_2 = \nu/(\alpha_2+\nu)$, which, combining with the recursion for $k \geq 3$ gives the product solution

$$c_k = c_1\,\frac{\nu-1}{\alpha_k}\prod_{j=2}^{k}\left(\frac{\alpha_j}{\alpha_j+\nu-1}\right). \tag{8}$$

For an explicit solution, we need the analytic form for α_k, which requires the probabilities f_k and t_k. For redirection probability $r(a,b) = 1 - b^{-\lambda}$, the quantities f_k and t_k reduce to

$$f_k = \sum_{b\geq 1}\frac{(1-b^{-\lambda})N(k,b)}{N_k} \equiv 1 - \langle b^{-\lambda}\rangle\,, \quad t_k = \sum_{a\geq 1}\frac{(1-k^{-\lambda})N(a,k)}{(k-1)N_k} = 1 - k^{-\lambda}\,, \tag{9}$$

where we use the sum rule $\sum_{a\geq 1} N(a,k) = (k-1)N_k$. We now combine Eq. (9) with $\alpha_k = (k-1)t_k + 1 - f_k$, to give $\alpha_k = k - k^{1-\lambda} + k^{-\lambda} - f_k \to k$ in the large-k limit. Finally, using $\alpha_k \sim k$ in the product solution (8) gives the asymptotic behavior

$$c_k \sim c_1\,\frac{\nu-1}{k}\prod_{j=2}^{k}\left(\frac{j}{j+\nu-1}\right) \sim k^{-\nu}\,. \tag{10}$$

Thus the degree distribution exhibits anomalous scaling, $N_k \sim N^{\nu-1}/k^{\nu}$, with $\nu < 2$, as given in (1).

Numerical simulations show that the exponent ν is a decreasing function of λ (Fig. 4). For $\lambda \to 0$, enhanced redirection becomes equivalent to random attachment,

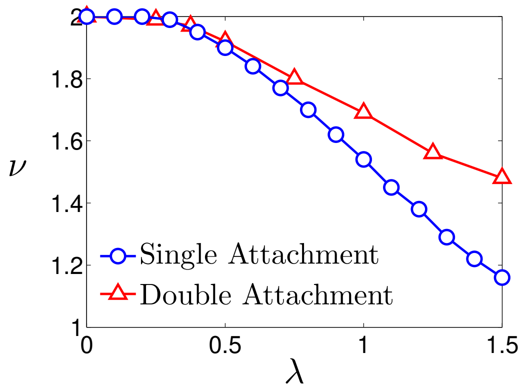

Figure 4. Degree distribution exponent ν versus λ for enhanced redirection with single attachment ($\circ$) and double attachment ($\triangle$). Each data point is determined from fits of N_k versus N, as in Figs. 3(a) and 11.

for which the degree distribution is extensive $N_k \sim N$ and $\nu \to 2$. As λ increases, attachment to a single node becomes progressively more likely and $\nu \to 0$. We also checked that the exponent ν is not affected by different initial conditions such as an initial loop of different sizes. However, finer details of the degree distribution, such as the probability distribution for the maximal degree and the number of core nodes, do depend on the initial condition.

One of the visually striking features of enhanced redirection networks is that they display large fluctuations from realization to realization, as are apparent from the examples in Fig. 2. To quantify these fluctuations, let us study $P(N_k)$, the distributions of the number of nodes of fixed degree k. For networks that are grown by preferential attachment, this distribution becomes progressively sharper as N increases [23], as long as the degree is not close to it maximal value. Thus the *average* number of nodes of a given degree can be regarded as the set of variables that fully characterizes the degree distribution. It is only the nodes of the highest degree that fail to self average [30].

In contrast, for enhanced redirection networks, essentially all geometrical features are non self-averaging, as illustrated by the distributions of $\mathcal{C}/N^{\nu-1}$, $N_2/N^{\nu-1}$, $N_3/N^{\nu-1}$, etc., which do not sharpen as N increases (Fig. 5). Since the number of core nodes $\mathcal{C}$ and the number of nodes of fixed degree N_k for $k \geq 2$ all scale as $N^{\nu-1}$ (Eq. (39)), scaled distributions of $N_k/N^{\nu-1}$ and $\mathcal{C}/N^{\nu-1}$ would progressively sharpen as N increases if self-averaging holds. The lack of self-averaging implies a sensitive dependence on initial conditions where events early in the evolution have lasting effects on the network structure. Surprisingly, the ratios $N_k/\mathcal{C}$ *are* self-averaging for $k \geq 2$, as the distributions $N_k/\mathcal{C}$ do sharpen as N increases (Fig. 5). The self-averaging of these ratios suggests that the degree distributions *given* a value of $\mathcal{C}$ are statistically similar, even though the overall number of core nodes $\mathcal{C}$ varies widely between realizations.

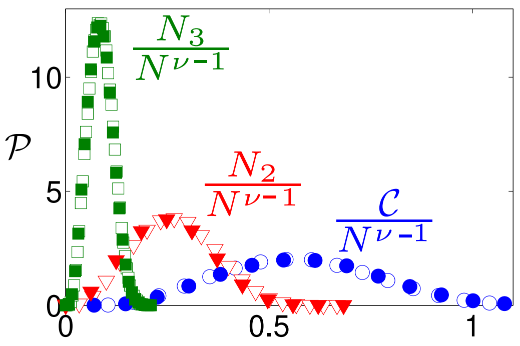

(a)

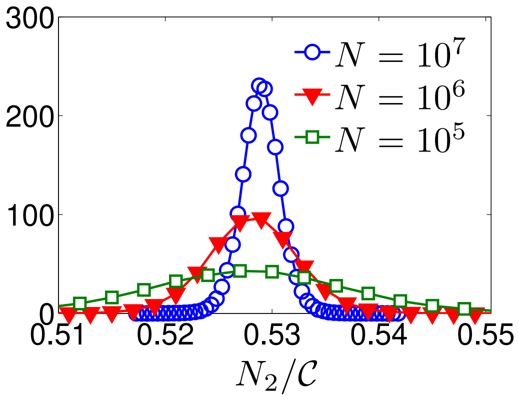

(b)

Figure 5. Probability densities in enhanced redirection for (a) $\mathcal{C}/N^{\nu-1}$, $N_2/N^{\nu-1}$, and $N_3/N^{\nu-1}$ for $N = 10^6$ (open symbols) and $N = 10^7$ nodes (closed symbols) and (b) $N_2/\mathcal{C}$. Data are based on 10^5 realizations with $\lambda = \frac{3}{4}$ and $\nu = 1.73$.

4. Singular Structures

Because of the tendency to connect to high-degree nodes, enhanced redirection networks tend to be dominated by one or a few high-degree nodes. In this section, we explore some of the consequences of this attraction to high-degree nodes.

4.1. Macrohubs

Macrohubs always arise when $\lambda > 0$, but they are easily detectable only when the exponent ν is notably smaller than 2. Figure 4 shows that this happens when $\lambda \gtrsim 0.4$, and in this range macrohubs are clearly observed in all network realizations. When the redirection parameter is small, $0 < \lambda < 0.4$, it may be necessary to grow the network to an astronomically large value of N to detect macrohubs with certainty.

There are usually many macrohubs, whose degree is proportional to N, as shown in Fig. 6(a). To estimate k_m, the degree of the m^{th} largest macrohub, we use the extremal criterion [31],

$$\sum_{k \geq k_m} N_k \sim m\,. \tag{11}$$

This equation merely states that there should be of the order of m nodes of degree k_m or larger. Thus k_m indeed gives an estimate for the value of the m^{th}-largest degree. Combining this criterion with the asymptotic $N_k \sim N^{\nu-1}/k^{\nu}$ from Eq. (1) gives

$$k_m \sim N/m^{1/(\nu-1)}. \tag{12}$$

The basic feature is that the degrees of macrohubs scale *linearly* with N. In contrast, for networks with an extensive degree distribution of the form $N_k \sim N/k^{\nu}$ and $\nu > 2$, the above extremal criterion gives the sub-linear growth: $k_m \sim (N/m)^{1/(\nu-1)}$.

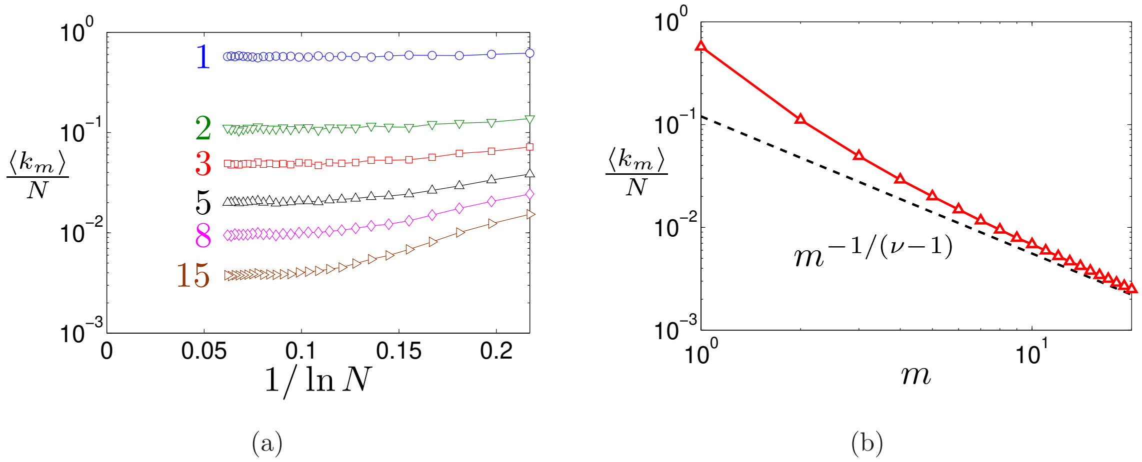

Figure 6. (a) The averages $\langle k_m \rangle/N$ versus $1/\ln N$ for selected m, illustrating that these values approach a finite fraction as $N \to \infty$. Each data point corresponds to 10^3 realizations. (b) $\langle k_m \rangle/N$ versus m for $N = 10^6$.

The degrees of the macrohubs substantially depends on the early stages of network growth, but once a set of macrohubs emerges (with degrees k_1, k_2, k_3, $\ldots$), the probability of attaching to a macrohub of degree k_m asymptotically approaches to k_m/N. This preferential attachment to macrohubs is similar to a Pólya urn process for filling an urn with balls of several colors [32, 33]. In the urn process, a ball is drawn at random from the urn and then replaced along with an additional matching-color ball. The different colors in the urn process correspond to different macrohubs in enhanced redirection. If there are k_m balls of the m^{th} color in an urn of N total balls, then the probability of choosing color m, and thus increasing k_m, is given by k_m/N. For the Pólya urn process, the ultimate fractions of balls of different colors do not self-average; the same is expected for the scaled degrees of macrohubs in enhanced redirection.

4.2. Star Graphs

Because of the tendency to link to high-degree nodes, it is possible that a star graph arises in which single node is connected to every other node of the network. As we now show, the probability for such a star to occur is non-zero for $\lambda > 1$. For the initial condition of a single node with a self loop, the star contains $N-1$ leaves, while the root node has degree $N+1$. The probability S_N to build such a star graph is

$$S_N(\lambda) = \prod_{n=1}^{N-1} \left\{ \frac{1}{n} + \frac{n-1}{n} \left[1 - (n+1)^{-\lambda} \right] \right\}. \tag{13}$$

The factor $\frac{1}{n}$ accounts for the new node attaching to the root in a network of n nodes, while the second term accounts for first choosing a leaf and then redirecting to the root.

As shown in Appendix A, the asymptotic behavior of (13) is

$$S_N(\lambda) \to \begin{cases} \mathcal{S}(\lambda) & \lambda > 1 \\ A/N & \lambda = 1 \\ \exp\left(-\frac{N^{1-\lambda}}{1-\lambda}\right) & 0 < \lambda < 1 \\ \frac{1}{(N-1)!} & \lambda = 0 \end{cases} \tag{14}$$

where $\mathcal{S}(\lambda) = \lim_{N\to\infty} S_N(\lambda)$ is a monotonically increasing function of λ when $\lambda > 1$ and $A = \pi^{-1}\sinh\pi \approx 3.676$.

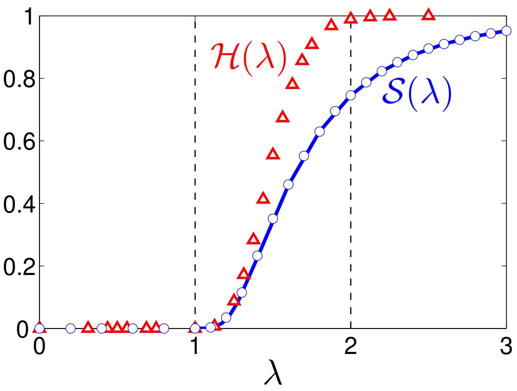

Figure 7. Probabilities for a star (○) and a hairball graph (△), $\mathcal{S}$ and $\mathcal{H}$, respectively. For each λ, the data are based on 10^5 realizations. The solid curve represents the numerical evaluation of the product in (13).

For $0 < \lambda \leq 1$, the probability of a star graph asymptotically approaches zero as $N \to \infty$. In this range, the network typically has many macrohubs with average sizes distributed according to Eq. (12). For $\lambda > 1$, a star graph occurs with a positive probability (Fig. 7), with a continuous phase transition at $\lambda = 1$. As shown in Appendix A, this phase transition has an infinite order because all derivatives of $\mathcal{S}(\lambda)$ vanish at $\lambda = 1$.

4.3. Size Distributions of Macrohubs

We now study the size distribution of the largest macrohub, the 2^{nd} largest macrohub, etc. By 'size' we mean the degree of a macrohub, so that there is no confusion between the size of the largest macrohub (a quantity characterizing one node) and the degree distribution which specifies the number of nodes of a fixed degree.

The degree k_m of the m^{th} largest macrohub scales linearly with the total number of nodes N, and therefore the corresponding size distribution $M_m(k_m, N)$ approaches the scaling form

$$M_m(k_m, N) \to \frac{1}{N}\,\mathcal{M}_m(x), \quad x = \frac{k_m}{N} \tag{15}$$

in the $N \to \infty$ limit. We do not know how to compute the scaling functions $\mathcal{M}_m(x)$, but some generic properties of these functions can be established without calculations. For instance, the scaling function $\mathcal{M}_m(x)$ vanishes when $x > 1/m$. Indeed, the m^{th}-largest macrohub has maximal degree $k_m = N/m$, which corresponds to the situation when the first m largest macrohubs all have equal maximally possible size N/m. Thus $\mathcal{M}_m(x)$ is singular at $x = 1/m$: $\mathcal{M}_m(x) \equiv 0$ when $x > 1/m$, and $\mathcal{M}_m(x) > 0$ when $x < 1/m$. Consider now the most interesting function $\mathcal{M}_1(x)$, which describes the scaled degree of the largest macrohub. It has a singularity at $x = 1$, and also a singularity at $x = 1/2$, as at this point the second-largest macrohub can emerge. Continuing this line of reasoning, we conclude that $\mathcal{M}_1(x)$ has infinitely many singularities that are located at $x = 1, 1/2, 1/3, 1/4, \ldots$. The emergence of these progressively weaker singularities is a generic feature and they arise in numerous examples including random walks, random maps, spin glasses, fragmentation, etc., which are characterized by the lack of self-averaging, see, e.g., [34–38]. Similarly, the scaling function $\mathcal{M}_m(x)$ has singularities at $x = 1/m, 1/(m+1), 1/(m+2), \ldots$.

The presence of infinitely many singularities (partly) explains why it is difficult to compute the scaling functions $\mathcal{M}_m(x)$. Fortunately, it is possible to probe the asymptotic behavior of $\mathcal{M}_m(x)$ near the maximal possible size $x = 1/m$. Consider the most interesting case of the largest macrohub. To determine the asymptotic behavior of $\mathcal{M}_1(x)$ in the $x \to 1$ limit, we notice that it can be extracted from the probability to build a star graph. Comparing (14) with (15) we find that in the marginal case of $\lambda = 1$

$$\mathcal{M}_1(1) = A = \frac{\sinh(\pi)}{\pi}\,, \tag{16}$$

while in the $0 < \lambda < 1$ range, the scaling function $\mathcal{M}_1(x)$ very rapidly vanishes near the upper limit:

$$\ln \mathcal{M}_1(x) \sim -(1-x)^{-(1-\lambda)} \qquad \text{when} \quad x \to 1. \tag{17}$$

The asymptotic behavior of $\mathcal{M}_2(x)$ in the $x \to \frac{1}{2}$ limit can be similarly extracted from the probability to build a $2-$star graph. We outline some of these calculations in the following subsection.

4.4. Hairballs

A slightly less singular variant of the star graph is what we term the “hairball” graph (Fig. 8). A hairball consists of multiple linked stars in which there are no nodes of degree 2. A star is thus a special case of hairball that consists of a single ball. The star probability is therefore always less than the hairball probability $\mathcal{H}(\lambda)$ (see also Fig. 7), and the latter appears to reach 1 for $\lambda > 2$. Thus enhanced redirection networks undergo two distinct phase transitions: (i) emergence of star graph when $\lambda > 1$ and (ii) the vanishing of nodes of degree 2 when $\lambda > 2$.

It is difficult to determine the hairball probability $\mathcal{H}(\lambda)$ analytically, as the number of high degree nodes and their degrees are unspecified. To gain insight, we consider

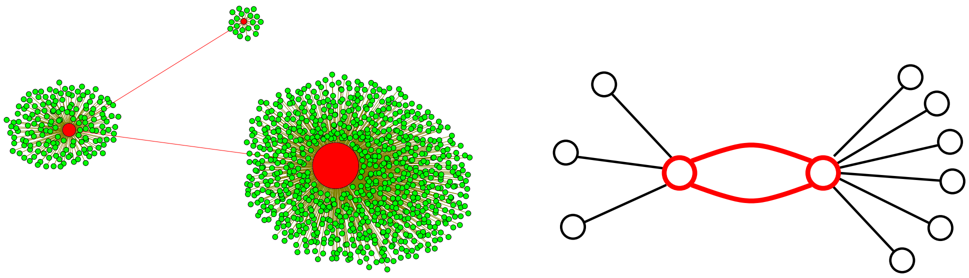

(a) (b)

Figure 8. (a) Example hairball network of $N = 10^3$ nodes generated by enhanced redirection with $\lambda = 2.5$. There are 3 core nodes (degree ≥ 2) with degrees $k = 819$, 163, and 21. (b) Idealized hairball graph $H_{m,n}$, with $(m, n) = (3, 6)$. The initial nodes and links are highlighted.

the more tractable probabilities for concrete types of hairballs. Let us start with the simplest hairball that contains two macrohubs. We also modify the initial condition to make the calculations more clean; namely, two nodes in a cycle of size 2 (Fig. 8(b)). A hairball with two macrohubs is thus a network where all nodes, apart from the two initial nodes, are leaves. Suppose that the network has reached the stage when one initial node is connected to m leaves and the other initial node is connected to n leaves. Let $H_{m,n}$ be the probability to reach such an (m, n) hairball. This hairball can arise from an $(m-1, n)$ or an $(m, n-1)$ hairball, which (by definition) occur with probabilities $H_{m-1,n}$ and $H_{m,n-1}$. Generally

$$H_{m,n} = g_{m-1,n}\, H_{m-1,n} + g_{n-1,m}\, H_{m,n-1}\,, \tag{18}$$

with coefficients g that depend on the redirection rule. For redirection probability $r(a, b) = 1 - b^{-\lambda}$

$$g_{m-1,n-1} = \frac{1}{m+n}\left[m - \frac{m}{(m+1)^{\lambda}} + \frac{1}{(n+1)^{\lambda}}\right]\,. \tag{19}$$

Instead of simulating enhanced redirection networks and looking for hairballs, we can use the recurrence (18) to calculate the exact values $H_{m,n}$ for any (m, n) starting from the obvious initial condition $H_{0,0} = 1$.

The recurrences (18) are readily solvable in the limit when either m or n vanishes. In this case

$$H_{N-2,0} = H_{0,N-2} = \frac{1}{2}\prod_{n=1}^{N-2}\left[1 - \frac{n-1}{n^{\lambda+1}}\right] \tag{20}$$

for $N \geq 3$. Hence the probability to generate the star graph, $S_N = H_{N-2,0} + H_{0,N-2}$, is

$$S_N(\lambda) = \prod_{n=1}^{N-2}\left[1 - \frac{n-1}{n^{\lambda+1}}\right]\,.$$

Using the same analysis as that used to derive Eq. (14), we find the asymptotic behaviors

$$S_N(\lambda) \to \begin{cases} \mathcal{S}(\lambda) & \lambda > 1\,, \\ B/N & \lambda = 1\,, \\ \exp\!\left(-\frac{N^{1-\lambda}}{1-\lambda}\right) & 0 < \lambda < 1\,, \end{cases} \tag{21}$$

with $\mathcal{S}(\lambda) = \prod_{n\geq 1}\left[1 - (n-1)/n^{\lambda+1}\right]$ and

$$B = \prod_{n=1}^{\infty}\left[1 + \frac{1}{n(n+1)}\right] = \frac{1}{\pi}\cosh\left(\frac{\pi\sqrt{3}}{2}\right) = 2.428189792\ldots$$

The differences between (14) and the above formulae stems from the different initial conditions.

The most interesting behavior arises when both m and n are large and comparable: $m \sim n \sim N$. In this regime we employ a continuum approach. We treat m and n as continuous variables and expand $H_{m-1,n}$ and $H_{m,n-1}$ in Taylor series to lowest order

$$H_{m-1,n} = H - \frac{\partial H}{\partial m}\,, \qquad H_{m,n-1} = H - \frac{\partial H}{\partial n}\,, \tag{22}$$

where $H \equiv H_{m,n}$. Substituting the expansions (22) into (18) and using (19), we recast the original recurrence into a partial differential equation that depends on λ. When $0 < \lambda < 1$, we obtain

$$m\,\frac{\partial H}{\partial m} + n\,\frac{\partial H}{\partial n} = -\left(m^{1-\lambda} + n^{1-\lambda}\right)H\,. \tag{23}$$

The controlling factor of the solution is given by

$$H_{m,n} \sim \exp\left[-\frac{m^{1-\lambda} + n^{1-\lambda}}{1-\lambda}\right], \qquad 0 < \lambda < 1\,. \tag{24}$$

To find the sub-leading factors, it would be necessary to refine (23) by keeping lower-order terms.

In the marginal case $\lambda = 1$, the partial differential equation becomes

$$m\,\frac{\partial H}{\partial m} + n\,\frac{\partial H}{\partial n} = -3H\,, \tag{25}$$

whose solution, which satisfies the necessary symmetry requirement $H_{m,n} = H_{n,m}$, is

$$H_{m,n} = \frac{C}{(mn)^{3/2}} \tag{26}$$

with some amplitude C that cannot be computed in the framework of the continuum approximation.

Setting $m = n = N/2$ (so that the corresponding total number of nodes in the network is $N+2$) we see that the probability of such $(N/2, N/2)$ graph scales as N^{-3}.

This is precisely the probability that the second-largest macrohub has the maximal possible size $N/2$. The scaling behavior (15) of the size distribution of the second-largest hub is compatible with the N^{-3} extremal behavior if

$$\mathcal{M}_2(x) \sim \left(\tfrac{1}{2} - x\right)^2 \qquad \text{when} \quad x \to \tfrac{1}{2}\,. \tag{27}$$

For $\lambda > 1$, the partial differential equation becomes

$$m\,\frac{\partial H}{\partial m} + n\,\frac{\partial H}{\partial n} = -H\,. \tag{28}$$

The remarkable feature of this equation is its universality (independence of λ) for large m and n. Solving (28) we get

$$H_{m,n} = \frac{C_2(\lambda)}{\sqrt{mn}}\,, \qquad \lambda > 1\,. \tag{29}$$

The multiplicative constant factor $C_2(\lambda)$ cannot be determined within the continuum framework. Setting again $m = n = N/2$ we find that the second largest macrohub has the maximal possible size $N/2$ with probability $2C_2(\lambda)/N$, which in conjunction with the scaling behavior (15) tells us that

$$\mathcal{M}_2\left(\tfrac{1}{2}\right) = 2C_2(\lambda) \qquad \text{when} \quad \lambda > 1\,. \tag{30}$$

Let us briefly discuss the general case of a hairball with p macrohubs. To simplify the analysis we again modify the initial condition by taking the initial network to be a cycle of p nodes. Generalizing the above analysis, we find that in the marginal case of $\lambda = 1$, the governing equation is

$$m_1\,\frac{\partial H}{\partial m_1} + \ldots + m_p\,\frac{\partial H}{\partial m_p} = -(2p-1)H\,, \tag{31}$$

whose solution is

$$H_{m_1,\ldots,m_p} = C_p\left(\prod_{j=1}^{p} m_j\right)^{-2+1/p}\,. \tag{32}$$

When $\lambda > 1$, the governing equation for H is

$$m_1\,\frac{\partial H}{\partial m_1} + \ldots + m_p\,\frac{\partial H}{\partial m_p} = -(p-1)H\,, \tag{33}$$

whose solution is

$$H_{m_1,\ldots,m_p} = C_p(\lambda)\left(\prod_{j=1}^{p} m_j\right)^{-1+1/p}\,. \tag{34}$$

Using these results we extract the asymptotic behavior of the scaled size distribution $\mathcal{M}_p(x)$ of the p^{th} largest macrohub in the $x \to \frac{1}{p}$ limit:

$$\mathcal{M}_p(x) \sim \begin{cases} \left(\frac{1}{p} - x\right)^{2p-2} & \lambda = 1, \\ \left(\frac{1}{p} - x\right)^{p-2} & \lambda > 1. \end{cases} \tag{35}$$

Finally when $\lambda < 1$, the asymptotic behavior of the scaled size distribution $\mathcal{M}_p(x)$ is extracted from (24), and its generalization to an arbitrary p, to give

$$\ln \mathcal{M}_p(x) \sim -\left(\tfrac{1}{p} - x\right)^{-(1-\lambda)}. \tag{36}$$

4.5. Root Node

To further appreciate the role of macrohubs let us now consider the evolution of the degree of the root node. We return to our default initial condition of a single root node that is linked to itself. Let $R(k,N)$ be the probability that the root has degree k in a network of N nodes. This probability was previously determined analytically for random attachment and linear preferential attachment networks [30], where it was shown that the root degree is broadly distributed for preferential attachment. For enhanced redirection, this probability obeys the difference equation

$$\begin{aligned} R(k,N+1) = &\left\{\frac{1}{N} + \frac{k-3}{N}\left[1 - \frac{1}{(k-1)^\lambda}\right]\right\} R(k-1,N) \\ &+ \left\{1 - \frac{1}{N} - \frac{k-2}{N}\left[1 - \frac{1}{k^\lambda}\right]\right\} R(k,N) \end{aligned} \tag{37}$$

with initial condition $R(2,1) = 1$. The first term gives the probability that the root has degree $k-1$ when the $(N+1)^{\text{th}}$ node connects to it, either directly or by redirection from the $k-3$ children of the root. The second term is the probability that the root has degree k and the $(N+1)^{\text{th}}$ node does *not* connect to the root. Iterating (37) numerically we obtain the numerical results for $R(k,N)$ shown in Fig. 9.

The behavior of the moments $\langle k^d \rangle_N = \sum_k k^d R(k,N)$ helps to shed light on the behavior of the root degree distribution $R(k,N)$. From Eq. (37), the mean degree evolves according to

$$N\langle k\rangle_{N+1} = (N+1)\langle k\rangle_N - \langle k^{1-\lambda}\rangle_N + 2\langle k^{-\lambda}\rangle_N - 1 \tag{38}$$

While this recurrence is not closed, we can drop the second term on the right-hand side of (38) as $N \to \infty$ because $\langle k^{1-\lambda}\rangle_N \ll \langle k\rangle_N$ (since $\lambda > 0$). The following terms are even smaller. Hence (38) simplifies to $\langle k\rangle_{N+1} \simeq \left(1 + \frac{1}{N}\right)\langle k\rangle_N$, from which $\langle k\rangle \sim N$. Similarly, the recurrence for the variance $\sigma_N = \langle k^2\rangle_N - \langle k\rangle_N^2$ shows that $\langle\sigma\rangle_{N+1} \simeq \left(1 + \frac{2}{N}\right)\langle\sigma\rangle_N$. This implies that $\langle\sigma\rangle \sim N^2$. Thus we conclude that the degree of the root is *not* self-averaging. The lack of self-averaging arises because the early evolution steps play a huge role in determining the root degree for large N.

Since the root degree is non self-averaging with $\langle k\rangle \sim N$, we anticipate that when $k, N \to \infty$, the probability distribution $R(k,N)$ admits the scaling form (Fig. 9)

$$R(k,N) = N^{-1}\Psi(x), \qquad x = \frac{k}{N} \tag{39}$$

When $\lambda \le 1$, the scaled distribution $\Psi(x)$ is a smooth function on $[0,1]$, but when $\lambda > 1$, $\Psi(x)$ additionally contains a singular component $\mathcal{R}(\lambda)\delta(x-1)$ that accounts for

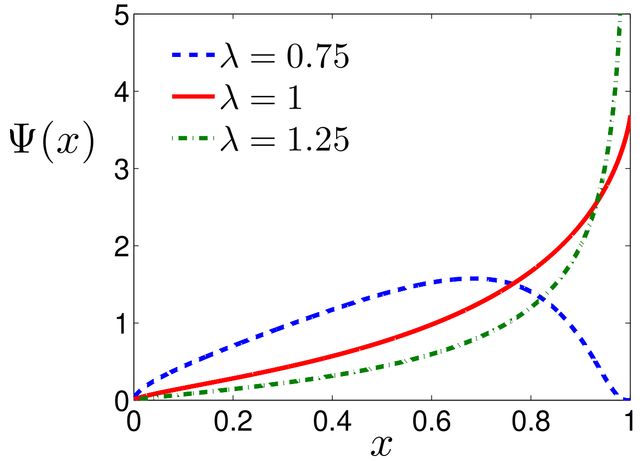

Figure 9. The scaling function from Eq. (39) for the root degree probability distribution.

the probability to create a star or a hairball about the root node. Therefore

$$\mathcal{R}(\lambda) \geq \mathcal{S}(\lambda) = \prod_{n=1}^{\infty}\left[1 - \frac{n-1}{n(n+1)^{\lambda}}\right]. \tag{40}$$

Consider the extreme behaviors at $x \to 1$. This limit essentially corresponds to the probability of forming the star. Thus for $\lambda = 1$ we expect $\Psi(1) = \pi^{-1}\sinh\pi \approx 3.676$. This agrees with simulation results. Further, $\Psi(1) = 0$ for $\lambda < 1$; more precisely, the scaling function $\Psi(x)$ near $x = 1$ is essentially the same as the scaling function $\mathcal{M}_1(x)$ describing the largest macrohub, Eq. (17). Hence $\ln\Psi(x) \sim -(1-x)^{-(1-\lambda)}$ as $x \to 1$. This is also compatible with our numerical results.

To estimate the asymptotic behavior of $\Psi(x)$ for $x \to 0$, we have computed the probabilities that the root has the smallest possible degrees $k = 3$ and $k = 4$ (Appendix B). From these results we infer the asymptotic behavior

$$\Psi(x) \sim x^{1-3^{-\lambda}} \qquad \text{as} \quad x \to 0\,, \tag{41}$$

which is compatible with our numerical results.

5. Enhanced Redirection with Multiple Attachments

In our discussion thus far, each new node added to the network has a single outgoing link. The resulting network is therefore a tree, except for closed loops that were part of the initial condition. It is therefore worthwhile to check whether the many anomalous features of enhanced redirection still exist if we allow the out-degree of each node to be larger than 1 so that closed loops can be created.

For simplicity, we consider the attachment rule in which a new node makes exactly two connections to existing nodes of the network—double attachment. We choose the

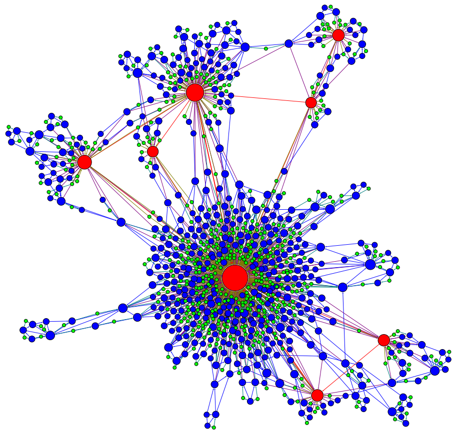

Figure 10. A network of $N = 10^3$ nodes which has been built by enhanced redirection with double attachment, Eq. (42) with $\lambda = 0.75$. The maximum degree in this example is $k_{\max} = 623$.

initial condition of a single node with two self-loops, so that the root node is its own parents. Nodes are added sequentially according to the following rules:

(i) The new node links to a randomly selected target node.

(ii) The new node links to one of the two parents of the target with probabilities

$$r_1(a,b) = \frac{a^\lambda}{a^\lambda + b^\lambda}, \qquad r_2(a,b) = \frac{b^\lambda}{a^\lambda + b^\lambda}, \tag{42}$$

where where a and b are the degrees of parent 1 and parent 2.

We choose these redirection probabilities so that attachment to a given parent becomes increasingly likely as its degree increases: $r_1(a,b) \to 1$ as $a \to \infty$ and $r_2(a,b) \to 1$ as $b \to \infty$. Figure 10 shows a typical network that has been generated by rules (i) and (ii) with $\lambda = 0.75$.

5.1. Degree Distribution

The two links created by each new node arise from two qualitatively different mechanisms. One link arises by random attachment, a mechanism that leads to the random recursive tree. The second link is to one of two parents, and it is selected via enhanced redirection which, as we have shown earlier, leads to a broad and non-extensive degree distribution, $N_k \sim N^{\nu-1}/k^\nu$ with $\nu < 2$. Because of the competition between these two mechanisms, one may anticipate that N_k scales linearly with N for sufficiently small k, while for large k the degree distribution N_k scales as $N^{\nu-1}$ with $\nu < 2$. This is indeed the case, as illustrated in Fig. 11.

To understand how two different scaling regimes emerge, we study the master equation that governs N_k (compare with Eq. (4)):

$$\frac{dN_k}{dN} = \left[\frac{N_{k-1}}{N} - \frac{N_k}{N}\right] + \left[\frac{\tau_{k-1}(k-3)N_{k-1}}{N} - \frac{\tau_k(k-2)N_k}{N}\right] + \delta_{k,2}\,. \tag{43}$$

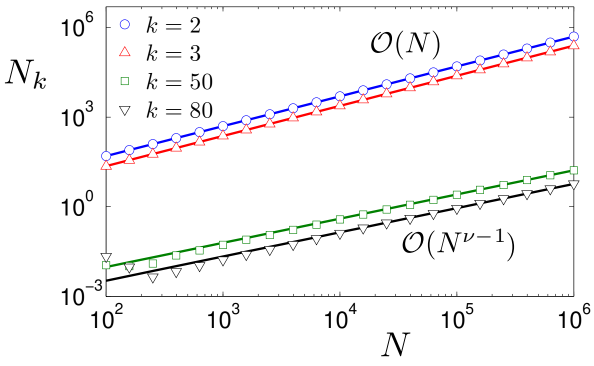

Figure 11. N_k versus N for degrees $k = 2$, 3, and degrees $k = 50$, 80 for $\lambda = 0.75$. The lines indicate the scaling $N_k \sim N$ and $N_k \sim N^{\nu-1}$ with $\nu = 1.8$.

The terms in the first set of brackets account for attachment to a randomly-selected target. Similarly, the terms in the second set of brackets account for redirection. Here

$$\tau_k = \sum_b \frac{r_1(k,b)N(k,b)}{(k-2)N_k}, \tag{44}$$

is the probability that an incoming node attaches to the degree-k parent of a random target, where $N(a,b)$ is the number of nodes with parents of degree a and b. Thus τ_k is the probability of redirection to a degree-k parent averaged over all $(k-2)N_k$ children of this parent node. In (43), the expression $\tau_k(k-2)N_k/N$ gives the probability that the incoming node initially targets one of the $(k-2)N_k$ children of a node of degree k and then redirects to this parent. The term $\delta_{k,2}$ accounts for each newly-created node has degree 2.

To determine N_k, we separately analyze Eq. (43) for small and for large k. When k is small, we make the ansatz $N_k = c_k N$ and substitute into Eq. (43). Rearranging, we find the recursion relation for c_k for $k > 2$:

$$c_k = \frac{1+(k-3)\tau_{k-1}}{2+(k-2)\tau_k} c_{k-1}\,, \tag{45}$$

while $c_2 = \frac{1}{2}$. This recursion has the product solution

$$c_k = \frac{1}{2^{k-1}} \prod_{j=3}^{k} \frac{1+(j-3)\tau_{j-1}}{1+(j-2)\tau_j/2}\,. \tag{46}$$

Since redirection to a low degree parent is unlikely, we approximate the redirection probability as $\tau_k = 0$ for small k. With this approximation, the product in Eq. (46) equals to 1, and the degree distribution reduces to $N_k \approx N/2^{(k-1)}$.

For large k, we substitute the non-extensive scaling ansatz $N_k = c_k N^{\nu-1}$ into Eq. (43), and rearrange to obtain the recursion

$$c_k = \frac{1+(k-3)\tau_{k-1}}{\nu+(k-2)\tau_k} c_{k-1}\,. \tag{47}$$

This gives the product solution

$$c_k = c_\ell \prod_{j=\ell+1}^{k} \frac{1+(j-3)\tau_{j-1}}{\nu+(j-2)\tau_j}, \tag{48}$$

where ℓ is the degree above which the non-extensive scaling ansatz is valid. In the limit of large k, we approximate $\tau_k = 1$ in Eq. (48)because the probability of redirection to a high-degree parent node approaches 1. This gives the asymptotic behavior

$$c_k = c_\ell \prod_{j=\ell+1}^{k} \frac{j-2}{j-2+\nu} \sim k^{-\nu}. \tag{49}$$

Combined with the non-extensive ansatz, the degree distribution for large k is $N_k \sim N^{\nu-1}/k^\nu$. In the above derivation, the precise value of ℓ only affects c_k up to a multiplicative factor but not the scaling behavior at large k.

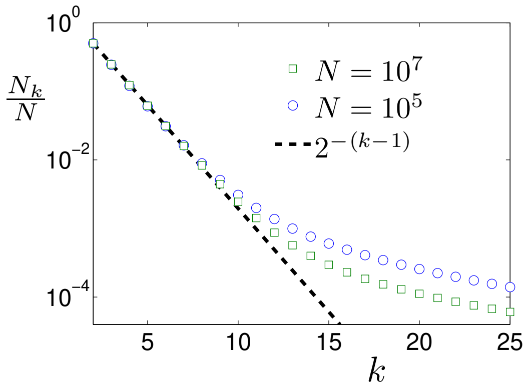

(a)

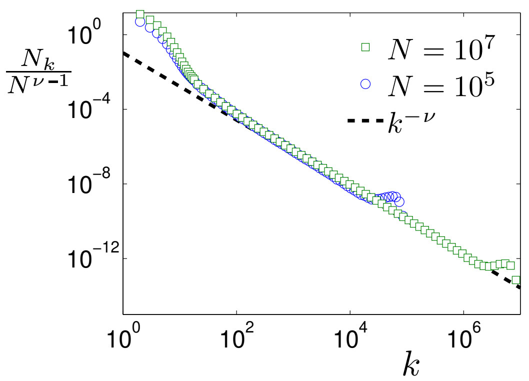

(b)

Figure 12. The degree distribution for double attachment with $\lambda = 0.75$ and $\nu = 1.8$ for $N = 10^5$, 10^6, and 10^7. In (a), the scaled degree distribution N_k/N is plotted to show the data collapse for small k. Similarly, (b) plots $N_k/N^{\nu-1}$ show the data collapse at large k.

We now define the crossover degree k^* as the value that separates the small-k extensive scaling regime from the large-k non-extensive regime. To estimate k^*, we find the value at which N_k in the small- and large-k approximations coincide. This leads to the transcendental equation $N/2^{(k^*-1)} = N^{\nu-1}/(k^*)^\nu$, whose solution gives $k^* \sim \ln N$ to lowest order in N.

To summarize, the limiting degree distributions are

$$N_k = \begin{cases} N/2^{(k-1)} & k \ll k^*, \\ cN^{\nu-1}/k^\nu & k \gg k^*, \end{cases} \tag{50}$$

with c a constant. As shown in Fig. 12, the agreement between this prediction and the degree distribution from Monte Carlo simulations is excellent. The double attachment rule also produces many macrohubs whose degrees grow linearly with N and also obey the same scaling behavior (12) as in single-attachment enhanced redirection.

5.2. Clustering Coefficient

The new feature of double attachment is that the resulting network contains closed loops. A basic question about this type of network is whether it is homogeneous or highly clustered. We measure the level of clustering by the *local clustering coefficient* $C_i(k)$ [7] for a given node i of degree k. This quantity is defined as the ratio of the actual number of links between the neighbors of node i to the $k(k-1)/2$ possible links between these neighbors if they were all connected. For the complete graph, the local clustering coefficient equals 1 for every node, while in a tree network the local clustering coefficient is everywhere zero.

To compute the local clustering coefficient for double attachment networks, consider an arbitrary node i with degree k. There are two ways that attachment can occur to this node: (i) a new node can attach directly to node i and to one of its parents, or (ii) a new node can attach to one of the $k-2$ children of node i and to node i itself. In either case, the degree of node i increases by one and the number of links between the neighbors of node i also increase by one. When node i is first created it necessarily has degree 2 and a single link between its neighbors. Thus when node i reaches degree k, it will have $k-1$ links between its neighbors. Therefore its clustering coefficient is $C_i(k) = (k-1)/[k(k-1)/2] = 2/k$. This $1/k$ scaling of the local clustering coefficient is seen in many real-world networks [39–42].

The average local clustering coefficient is therefore

$$\langle C_i \rangle = \frac{1}{N}\sum_{k=2}^{2N} C(k) N_k = \frac{2}{N}\sum_{k=2}^{2N}\frac{N_k}{k}\,. \tag{51a}$$

We partition the sum according to whether k is smaller or greater than k^* using Eq. (50). This gives

$$\langle C_i \rangle = \sum_{k=2}^{k^*}\frac{1}{2^{(k-2)}\,k} + N^{\nu-2}\sum_{k=k^*+1}^{2N}\frac{2}{k^{\nu+1}}\,, \tag{51b}$$

with $k^* \sim \ln N$ the cutoff between the two scaling regimes. As $N\to\infty$, the second term vanishes, because $\nu < 2$, and the first term asymptotically approaches

$$\langle C_i \rangle \to \sum_{k=2}^{\infty} 2^{-(k-2)} k^{-1} = 4\ln 2 - 2 = 0.77258\ldots \tag{51c}$$

This large value for this coefficient value indicates a highly clustered network. For comparison, empirical studies found $\langle C_i \rangle = 0.79$ for actor collaboration networks [39], 0.68 for co-authorship networks [40], and 0.14 for blogging networks [41]. By contrast, the Erdős-Rényi random graphs have a vanishing mean local clustering coefficient; more precisely it decreases with N according to $\langle C_i \rangle \sim N^{-1}$ [42].

6. Conclusion

Enhanced redirection is an appealing mechanism that produces networks with a variety of unusual features, including the existence of multiple macroscopic hubs, anomalous scaling of the degree distribution, and lack of self-averaging. Unlike other models that produce macrohubs, enhanced redirection is based solely on local growth rules and does not assume intrinsic differences between nodes. Networks grown by enhanced redirection are highly disperse and typically consist of a set of loosely-connected macrohubs that is reminiscent of airline route networks [7, 21, 24–26].

Intriguingly, the degree distribution decays more slowly than k^{-2}. Such an anomalously slow decay is mathematically consistent with a finite average degree only if the number of nodes of fixed degrees scales sub-linearly with the number of nodes N. Enhanced redirection may thus provide the mechanism that underlies the wide range of networks [27] whose degree distributions apparently decay more slowly than k^{-2}.

We also combined the enhanced redirection mechanism with the simplest random attachment to produce networks that contain closed loops. The resulting degree distribution exhibits an unusual combination of extensive and non-extensive scaling. The clustering coefficient in these networks is large, as is observed in many real networks, and thus this rule produces highly-clustered network with numerous macrohubs.

This research was partially supported by the AFOSR and DARPA under grant #FA9550-12-1-0391 and by NSF grant No. DMR-1205797.

Appendix A. Star Probability

To derive the asymptotic behaviors given in (14) we first re-write (13) as

$$S_N(\lambda) = \prod_{n=1}^{N-1} \left[1 - \frac{n-1}{n(n+1)^\lambda}\right]. \tag{A.1}$$

When $\lambda > 1$, the product on the right-hand side of (A.1) converges to

$$\mathcal{S}(\lambda) = \prod_{n=1}^{\infty} \left[1 - \frac{n-1}{n(n+1)^\lambda}\right]. \tag{A.2}$$

The probability $\mathcal{S}(\lambda)$ is clearly positive and an increasing function of $\lambda > 1$ (see also Fig. 7). Numerical evaluation of the product gives, for example, $\mathcal{S}(2) \approx 0.74562$, $\mathcal{S}(4) \approx 0.9884$, $\mathcal{S}(6) \approx 0.999$.

When $\lambda \leq 1$, the product on the right-hand side of (A.1) converges to zero as $N \to \infty$. Consider first the case where $0 < \lambda < 1$. We take the logarithm of (A.1) and expand the logarithm. Since the dominant contribution arises for large n, we can replace the sum by an integral to yield

$$\ln S_N(\lambda) = \sum_{n=1}^{N-1} \ln \left[1 - \frac{n-1}{n(n+1)^\lambda}\right] \sim -\int^N \frac{dn}{n^\lambda} = -\frac{N^{1-\lambda}}{1-\lambda}\,.$$

In the marginal case of $\lambda = 1$ we use $\prod_{1\leq n\leq N-1} [1-(n+1)^{-1}] = N^{-1}$ to rewrite Eq. (A.1) at $\lambda = 1$ as

$$NS_N(1) = \prod_{n=1}^{N-1} \frac{1 - \frac{n-1}{n(n+1)}}{1 - \frac{1}{n+1}} = \prod_{n=1}^{N-1} \left[1 + n^{-2}\right]. \tag{A.3}$$

The last product converges to $A = \pi^{-1}\sinh\pi$ as $N \to \infty$ [43]. In the extreme case of $\lambda = 0$, we simplify Eq. (13) to give $S_N(0) = 1/(N-1)!$. These give the results summarized in Eq. (14). It is worth emphasizing that the third line in (14), $\exp[-N^{1-\lambda}/(1-\lambda)]$ represents only the controlling factor in the asymptotic behavior. Subdominant, and possibly less singular contributions as $N \to \infty$ have been neglected.

The precise behavior of $\mathcal{S}(\lambda)$ in the $\lambda - 1 \to 0^+$ limit can be extracted from (A.2). Taking the logarithm of the infinite product for $\mathcal{S}(\lambda)$, expanding the logarithm, and separating the terms that converge and diverge as $\lambda \downarrow 1$, one gets

$$\ln \mathcal{S}(\lambda) = -\zeta(\lambda) + 2 + \sum_{n\geq 1}\left(\tfrac{n}{(n+1)(n+2)} + \ln\Big[1 - \tfrac{n}{(n+1)(n+2)}\Big]\right) + \mathcal{O}(\lambda - 1)\,.$$

Recalling the asymptotic behavior of the zeta function, $\zeta(\lambda) = (\lambda-1)^{-1} + \gamma + \mathcal{O}(\lambda-1)$, where $\gamma \approx 0.5772$ is Euler's constant, we conclude that

$$\mathcal{S}(\lambda) \simeq \exp\!\Big(-\frac{1}{\lambda-1} + C\Big)\,, \tag{A.4}$$

with

$$C = 2 - \gamma + \sum_{n\geq 1}\left[\tfrac{n}{(n+1)(n+2)} + \ln\Big(1 - \tfrac{n}{(n+1)(n+2)}\Big)\right] \approx 1.3018\,.$$

Let us now compute the probability to form the star for the model with redirection probability $r(a,b) = a^\lambda/(a^\lambda + b^\lambda)$. One gets

$$S_N(\lambda) = \prod_{n=1}^{N-1}\left[1 - \frac{n-1}{n}\,\frac{1}{1+(n+1)^\lambda}\right]$$

from which

$$S_N(\lambda) \to \begin{cases} \widehat{\mathcal{S}}(\lambda) & \lambda > 1 \\ \widehat{A}/N & \lambda = 1 \\ \exp\!\Big(-\frac{N^{1-\lambda}}{1-\lambda}\Big) & 0 < \lambda < 1 \\ \frac{N}{2^{N-1}} & \lambda = 0 \end{cases} \tag{A.5}$$

where $\widehat{\mathcal{S}}(\lambda) = \prod_{n\geq 1}\Big[1 - \frac{n-1}{n}\,\frac{1}{1+(n+1)^\lambda}\Big]$ and the amplitude $\widehat{A}$ is found by employing the same construction as that used for Eq. (A.3) to yield

$$\widehat{A} = \prod_{n=1}^{\infty}\left[1 + \frac{2n+1}{n^2(n+2)}\right] = \frac{2}{\pi}\cosh\left(\frac{\pi\sqrt{3}}{2}\right) = 4.856379592\ldots$$

Again, the third line in Eq. (A.5) represents only the controlling factor in the asymptotic behavior in which subdominant contributions as $N \to \infty$ have been neglected.

The predictions (14) and (A.5) for the two models (3) are qualitatively the same for the same values of λ. More precisely, qualitatively different networks emerge only in the extreme case $\lambda = 0$ which is not interesting to us as our goal is to study *enhanced* redirection. (When $\lambda = 0$, the first model in (3) leads to uniform attachment without redirection, the process that generates recursive random trees, while the second model in (3) leads to constant redirection probability $r = 1/2$ which is equivalent to strictly linear preferential attachment process.)

Appendix B. Smallest Root Degree

The minimal possible degree of the root is $k = 3$ when $N \geq 2$. Using (37) we get

$$R(3, N+1) = \left[1 - \frac{2 - 3^{-\lambda}}{N}\right] R(3, N)\,. \tag{B.1}$$

Starting from $R(3, 2) = 1$ and iterating (B.1) we find

$$R(3, N) = \frac{\Gamma(N - 2 + 3^{-\lambda})}{\Gamma(N)\,\Gamma(3^{-\lambda})} \simeq \frac{1}{\Gamma(3^{-\lambda})}\, N^{-2+3^{-\lambda}}\,. \tag{B.2}$$

Let us now probe the behavior of the second smallest degree $k = 4$. Using (37) we obtain the recurrence

$$R(4, N+1) = \frac{2 - 3^{-\lambda}}{N}\, R(3, N) + \left[1 - \frac{3 - 2^{1-2\lambda}}{N}\right] R(4, N)\,. \tag{B.3}$$

Making the substitution

$$R(4, N) = \frac{\Gamma(N - 3 + 2^{1-2\lambda})}{\Gamma(N)}\, U(N)\,, \tag{B.4}$$

and using (B.2) we recast (B.3) into a simple recursion

$$U(N+1) = U(N) + \frac{2 - 3^{-\lambda}}{\Gamma(3^{-\lambda})} \cdot \frac{\Gamma(N - 2 + 3^{-\lambda})}{\Gamma(N - 2 + 2^{1-2\lambda})}\,,$$

from which

$$U(N) = \frac{2 - 3^{-\lambda}}{\Gamma(2^{1-2\lambda})} + \frac{2 - 3^{-\lambda}}{\Gamma(3^{-\lambda})} \sum_{j=1}^{N-3} \frac{\Gamma(j + 3^{-\lambda})}{\Gamma(j + 2^{1-2\lambda})}\,. \tag{B.5}$$

Using Eqs. (B.4) and (B.5) one deduces the asymptotic behavior

$$R(4, N) \simeq \frac{1}{\Gamma(3^{-\lambda})} \, \frac{2 - 3^{-\lambda}}{1 + 3^{-\lambda} - 2^{1-2\lambda}}\, N^{-2+3^{-\lambda}}\,. \tag{B.6}$$

The asymptotic behaviors (B.2) and (B.6) exhibit the same dependence on the number of nodes N. Generally, $R(k, N) \sim N^{-2+3^{-\lambda}}$ when $N \gg 1$ and k is kept finite. This, in conjunction with the scaling form (39), leads to the small-x behavior given in (41) for the scaled root degree distribution.

[1] G. U. Yule, Phil. Trans. Roy. Soc. B **213**, 21 (1925).
[2] H. A. Simon, Biometrika **42**, 425 (1955).
[3] A.-L. Barabási and R. Albert, Science **286**, 509 (1999).
[4] P. L. Krapivsky, S. Redner, and F. Leyvraz, Phys. Rev. Lett. **85**, 4629 (2000).
[5] S. N. Dorogovtsev, J. F. F. Mendes, and A. N. Samukhin, Phys. Rev. Lett. **85**, 4633 (2000).
[6] S. N. Dorogovtsev and J. F. F. Mendes, *Evolution of Networks: From Biological Nets to the Internet and WWW* (Oxford University Press, Oxford, UK, 2003).
[7] M. E. J. Newman, *Networks: An Introduction* (Oxford University Press, Oxford, 2010).
[8] A. Fabrikant, E. Koutsoupias, and C. H. Papadimitriou, *Automata, Languages and Programming*, Lecture Notes in Computer Science, **2380**, 110, Springer, Berlin, 2002).
[9] V. Colizza, J. R. Banavar, A. Maritan, and A. Rinaldo, Phys. Rev. Lett. **92**, 198701 (2004).
[10] M. Barthelemy, Phys. Rept. **499**, 1 (2011).
[11] F. Papadopoulos, M. Kitsak, M. Ángeles Serrano, M. Boguñá, and D. Krioukov, Nature **489**, 537 (2012).
[12] J. Kleinberg, R. Kumar, P. Raghavan, S. Rajagopalan, and A. Tomkins, in: *Proceedings of the International Conference on Combinatorics and Computing*, Lecture Notes in Computer Science, Vol. 1627, pp. 1-18 (Springer-Verlag, Berlin, 1999).
[13] P. L. Krapivsky and S. Redner, Phys. Rev. E **63**, 066123 (2001).
[14] A. Vázquez, Phys. Rev. E **67**, 056104 (2003).
[15] H. Rozenfeld and D. ben-Avraham, Phys. Rev. E **70**, 056107 (2004).
[16] P. L. Krapivsky and S. Redner, Phys. Rev. E **71**, 036118 (2005).
[17] R. Lambiotte and M. Ausloos Europhys. Lett. **77**, 58002 (2007).
[18] E. Ben-Naim and P. L. Krapivsky, J. Stat. Mech. P06004 (2010).
[19] A. Gabel and S. Redner, J. Stat. Mech. P02043 (2013).
[20] P. L. Krapivsky and D. Krioukov, Phys. Rev. E **78**, 026114 (2008).
[21] R. F. i Cancho and R. V. Solé, *Statistical Mechanics of Complex Networks*, no. 625 in Lecture Notes in Physics, p. 114, Springer, Berlin (2003).
[22] G. Bianconi and A.-L. Barábasi, Phys. Rev. Lett. **86**, 5632 (2001); G. Bianconi and A.-L. Barábasi, Europhys. Lett. **54**, 436 (2001).
[23] P. L. Krapivsky and S. Redner, Comput. Netw. **39**, 261 (2002).
[24] D. L. Bryan and M. E. O'Kelly, J. Regional Science, **39**, 275 (1999).
[25] J. J. Han, N. Bertain, T. Hao, D. S. Goldberg, G. F. Berriz, L. V. Zhang, D. Dupay, A. J. M. Walhout, M. E. Cusick, F. P. Roth, and M. Vidal, Nature **430**, 88 (2004).
[26] R. Guimera, S. Mossa, A. Turtschi, and L. A. N. Amaral, Proc. Natl. Acad. Sci. USA **102**, 7794 (2005).
[27] J. Kunegis, M. Blattner, and C. Moser, arXiv:1303.6271.
[28] P. L. Krapivsky and S. Redner, J. Phys. A **35**, 9517 (2002).
[29] A. Gabel, P. L. Krapivsky, and S. Redner, Phys. Rev. E **88**, 050802 (2013).
[30] P. L. Krapivsky and S. Redner, Phys. Rev. Lett. **89**, 258703 (2002).
[31] E. J. Gumbel, *Statistics of Extremes* (Columbia University Press, New York, 1958).
[32] F. Eggenberger and G. Pólya, Z. Angew. Math. Mech. **3**, 279 (1923).
[33] N. Johnson and S. Kotz, *Urn Models and Their Applications: An Approach to Modern Discrete Probability Theory*, (Wiley, New York, 1977); H. M. Mahmoud, *Pólya Urn Models* (Chapman & Hall, London, 2008).
[34] B. Derrida and H. Flyvbjerg, J. Phys. A **20**, 5273 (1987); J. Physique **48**, 971 (1987); B. Derrida and D. Bessis, J. Phys. A **21**, L509 (1988).
[35] P. G. Higgs, Phys. Rev. E **51**, 95 (1995).
[36] L. Frachebourg, I. Ispolatov, and P. L. Krapivsky, Phys. Rev. E **52**, R5727 (1995).
[37] B. Derrida and B. Jung-Muller, J. Stat. Phys. **94**, 277 (1999).
[38] P. L. Krapivsky, I. Grosse, and E. Ben-Naim, Phys. Rev. E **61**, R993 (2000); P. L. Krapivsky, E. Ben-Naim, and I. Grosse, J. Phys. A **37**, 2863 (2004).

[39] D. Watts and S. H. Strogatz, Nature **393**, 440 (1998).
[40] F. J. Acedo, C. Barroso, C. Casanueva, and J. L. Galán, J. Management Studies **43**, 970 (2006).
[41] F. Fu, L. Liu, and L. Wang, Physica A **387**, 675 (2008).
[42] E. Ravasz and A.-L. Barabási, Phys. Rev. E **67**, 026112 (2003).
[43] M. Abramowitz and A. Stegun, *Handbook of Mathematical Functions* (Dover, New York, 1965).